Kr Extended X-ray Absorption Fine Structure Study of Endohedral Kr@C_{60}

S. Ito,[†] A. Takeda,[†] T. Miyazaki,[†] Y. Yokoyama,[†] M. Saunders,[‡] R. J. Cross,[‡] H. Takagi,[†] P. Berthet,[§] and N. Dragoe*[,§]

Department of Advanced Materials Science, The University of Tokyo, 277-8562 Chiba, Japan, Department of Chemistry, Yale University, New Haven, Connecticut 06520-8107, and Laboratoire de Physico-Chimie de l'Etat Solide, ICMMO, Université Paris-Sud, Bâtiment 414, UMR 8648-CNRS, Orsay 91405, France

Received: October 14, 2003; In Final Form: December 5, 2003

An EXAFS study has been performed at the K-edge of Kr atoms in C_{60} cages. Single-scattering peaks yield the radius of the C_{60} cage as "seen" by the inserted krypton atom. Peaks assigned to multiple scattering, located from 4 to 5 Å in the radial distribution functions, gave an indication about a rotation of the cage, in the solid, similar to that proposed for empty C_{60}.

Introduction

One of the interesting features of fullerene is that it has a hollow space in the carbon cage;[1] it is therefore appealing to insert in this space other atoms or molecules and then study the properties of these new species named endohedral fullerenes. From the viewpoint of electronic interactions, endohedral fullerenes can be divided in two groups. One group we can classify as the metal endohedral fullerenes, for instance, fullerenes with La, Y atoms inserted in C_{82}, and so forth.[2,3] The characteristic of this class is the existence of an electronic charge transfer from the inserted atom to the fullerene cage. It is common for this category that the inserted atom lies close to the fullerene cage because of the strong Coulombic interaction.[4] Because of this charge transfer, the properties of endohedral compounds, including retention time in high-performance liquid chromatography (HPLC), are different from those of empty fullerenes; hence, their purification is usually straightforward.[5,6] The second category of endohedral fullerenes is that of the noninteracting intercalants such as N,[7] P,[8] or noble gas atoms.[9,10] These endohedral fullerenes show little or no charge transfer to the cage, and the inserted atom remains in the center of the cage. Because these endohedral fullerenes have no charge transfer, the properties of these endohedral fullerenes are almost the same as those of empty fullerenes. Therefore, these endohedral fullerenes can be used as tracers, for instance by ^{3}He-NMR for ^{3}He@C_{60},[11,12] by electron paramagnetic resonance (EPR) for N@C_{60}, or by measuring the isotopic-like effects on their properties by comparison with empty fullerenes. On the other hand, their similarity with the empty cages makes their purification very difficult.[13,14] However, we separated about 1 mg of Kr@C_{60} of 99% purity (using HPLC). This sample has been analyzed by several spectroscopic methods; we describe here the extended X-ray absorption fine structure (EXAFS) results for Kr@C_{60} obtained at the Kr K-edge. EXAFS is a local probe sensitive to the environment of the absorbing atoms, thus it gives important details about the structure as well as the dynamics of the system.

* Author to whom correspondence should be addressed.
[†] University of Tokyo.
[‡] Yale University.
[§] Université Paris-Sud.

Experimental Details

A C_{60} sample containing about 1% Kr@C_{60} was synthesized by a high-pressure, high-temperature technique as described earlier.[10] HPLC separation of this sample was performed on a JASCO GULLIVER 1500 instrument equipped with recycling, an automatic injector, and a diode array detector (300−900 nm). The column used was a Cosmosil Buckyprep (20 × 250 mm Nakalai Tesque, Kyoto, Japan). The flow rate was 20 mL/min of toluene with injection volumes of 5 mL; the separation was performed at 50 °C in order to decrease peak tailing. About 1 mg of 99% pure Kr@C_{60} sample was obtained by HPLC using a procedure involving recycling and sequential HPLC, similar to one reported previously.[14] This sample, in its polycrystalline form, was deposited from a CS_2 solution onto a Teflon sample holder.

EXAFS spectra were measured at the Kr K-edge at 300 K (RT sample) and at 80 K (LT sample) using the LURE-DCI synchrotron source (Orsay, France) operated at 1.85 GeV with a 250 mA positron current on the D42-XAS13 beam line. Experiments were performed in fluorescence mode from 14.2 to 14.8 keV with a 3 eV step using a Si (111) double-crystal monochromator; the calibration was obtained from the L_I absorption edge of a thin gold foil. The sample was not affected by the X-ray irradiation.

We recorded 20 scans at room temperature and 15 scans at 80 K; the data were then aligned in energy and merged. Experimental data were analyzed using the programs IFEFFIT[15] and FEFF8.[16]

Results and Discussion

Little work on Kr EXAFS data is available in the literature and, to the best of our knowledge, none for a well-defined Kr compound. Several works are known in general for gas, liquid, and solid Kr under high pressures[17] as well as for Kr dissolved in vitreous silica.[18] The availability of pure Kr@C_{60}, stable at room temperature, a novel type of a van der Waals molecule,[19] prompted us to perform a detailed analysis of its absorption properties at the Kr K-edge.

Figure 1a shows the EXAFS spectrum of the sample at low temperature, and Figure 1b shows the EXAFS signal extracted from these data in k-space ($k^2 = 2m_e(E - E_0)$ with $E_0 = 14322$

10.1021/jp037108w CCC: $27.50
Published on Web 02/14/2004

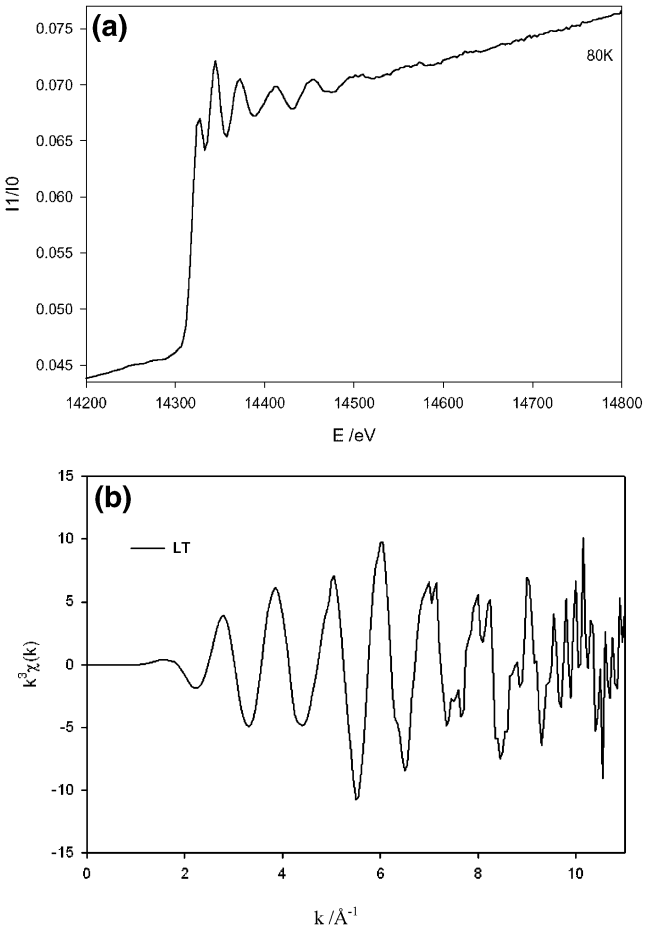

Figure 1. (a) X-ray absorption spectrum of Kr@C_{60}. (b) Kr@C_{60} EXAFS $k^3\chi(k)$ at 80 K.

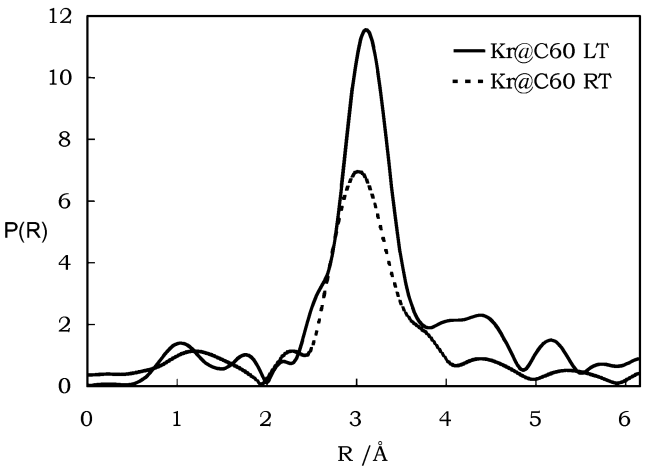

Figure 2. Fourier transform of $k^3\chi(k)$ experimental data of the LT and RT samples.

eV). Figure 2 shows the Kaiser−Bessel Fourier transform derived from the $k^3\chi(k)$ experimental data of the LT (from 1.8 to 10.1 Å^{-1}) and RT (from 1.6 to 9.2 Å^{-1}) samples. The large peak located at about 3 Å is assigned to the single-scattering paths from the Kr atom to the carbon atoms of the C_{60} cage which is known to have a radius close to 3.5 Å; the 0.5 Å difference between the position of the peak and the cage radius comes from the mean scattering phase shift of the photoelectron. For both data sets the peaks are located at the same position although their intensity is clearly lower at room temperature.

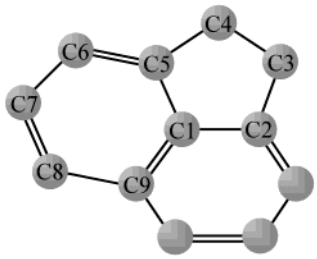

Figure 3. Fragment of the fullerene cage showing the different types of bonds.

TABLE 1: Scattering Paths and Amplitudes for Kr@C_{60} Calculated by FEFF8

path	degeneracy	distance (Å)	amplitude					
1	60	3.54	100	Kr	C1	Kr		
2	60	4.236	22.19	Kr	C1	C9	Kr	
3	120	4.265	40.44	Kr	C1	C2	Kr	
4	120	4.713	15.02	Kr	C1	C3	Kr	
5	240	4.77	27.43	Kr	C1	C6	Kr	
6	60	4.931	8.43	Kr	C1	C9	C1	Kr
7	120	4.96	10.44	Kr	C1	C7	Kr	
8	240	4.96	18.39	Kr	C1	C5	C6	Kr
9	120	4.99	14.64	Kr	C1	C2	C1	Kr
10	120	4.99	8.54	Kr	C1	C2	C3	Kr
11	240	5.323	12.98	Kr	C3	C9	Kr	
12	120	5.382	5.99	Kr	C2	C8	Kr	
13	240	5.408	5.58	Kr	C3	C1	C9	Kr
14	240	5.438	12.01	Kr	C1	C2	C5	Kr
15	240	5.438	8.87	Kr	C1	C2	C4	Kr
16	240	5.466	12.22	Kr	C1	C9	C2	Kr
17	240	5.466	6.74	Kr	C1	C9	C7	Kr
18	240	5.495	11.46	Kr	C1	C5	C9	Kr
19	240	5.495	4.42	Kr	C8	C1	C2	Kr
20	240	5.495	6.26	Kr	C5	C1	C8	Kr

At a first glance the intensity difference can be assigned to a thermal factor difference because no change in coordination geometry, or in the coordination number took place with temperature. The small peaks observed at larger distance, especially for the LT sample, are assigned to multiple scattering (MS) involving several carbon atoms. There is a rather important difference between the two samples in this region, the LT sample showing a double peak located from 3.8 to 4.7 Å. The diminution of the MS contributions at high temperature can be assigned to the rotation of the molecules and will be discussed later.

For the fitting of the RT and LT data, we employed the paths and amplitudes calculated by FEFF8. We used different models for the Kr@C_{60} crystal structure without noticing changes in the results obtained. This is due to the fact that all contributions come from the molecular structure: the distance between the Kr atom and an atom from the next neighboring C_{60} cage is about 7 Å; this is not in the range of our analysis. We note, however, that crystallographic data reported for C_{60} do not respect the icosahedral symmetry of C_{60}; the resulting cage is slightly distorted, and this leads to an artificial distribution of the distances for the first shell. To avoid this inconvenience, we used a molecular model of Kr@C_{60} obtained by ab initio calculations at the B3LYP/3-21G* level. This model has an I_h symmetry with 60 carbon atoms located at a distance of 3.54 Å from the Kr atom which was central. This distance is the same as the average one observed by single-crystal X-ray diffraction in a compound of Kr@C_{60}.[20] The possible paths to be considered in the calculations are listed in Table 1 and can be described as seen in Figure 3. Besides the single-scattering path at 3.54 Å, one can observe three-legged paths related to the nonequivalence of the C−C bonds in the hexagon ring of

TABLE 2: Results Obtained by Fitting the LT Sample (One Path), the LT Sample (Three Paths), the RT Sample (Three Paths), and the RT Sample (Three Paths with One Parameter Fixed[a])

	LT sample, one path		LT sample, three paths		RT sample, three paths		RT sample, three paths[a]	
fit	value	error	value	error	value	error	value	error
dE (eV)	−0.40	1.17	−2.73	0.73	−4.53	0.86	−5.12	0.99
R (Å)	3.552	0.015	3.540	0.007	3.537	0.009	3.537	0.011
σ^2 (Å^2)	0.007	0.002	0.009	0.001	0.009	0.001	0.013	0.000
S02_1	0.85	0.19	1.02	0.10	0.71	0.09	1.00*	
S02_2			1.19	0.24	0.71	0.21	1.20	0.29
χ^2	9.57		4.58		2.90		4.86	
R-factor	0.115		0.049		0.017		0.032	

[a] Marked by an asterisk.

the fullerenes: the Kr−C1−C9−Kr half-length is 4.236 Å whereas that of Kr−C1−C2−Kr is 4.265 Å. For the Kr−C1−C3−Kr path including a diagonal of the pentagon, there is a calculated distance of 4.713 Å, whereas for the small diagonal of a hexagon such as Kr−C1−C6−Kr this is 4.77 Å. From 4.9 Å the four-legged paths' contribution becomes significant as can be seen from Table 1.

For fitting we used the classical EXAFS formula for the ith path contribution:

$$k\chi_i(k) = (N_i/R_i^2)\exp(-2\sigma_i^2k^2)\exp(-2R_i/\lambda)|f_i(k)|\sin(2kR_i + \Phi_i)$$

where N_i is the number of the atoms in the path; in our case $N_i = S_0^2C_i$, where S_0^2 is the occupation factor and C_i is the number of equivalent paths, which are listed in Table 1 as the *degeneracy*. R_i is the path distance, σ_i^2 is a Debye−Waller factor, λ is the mean free path of the photoelectron, $|f_i(k)|$ is the scattering amplitude, and Φ_i is the total phase shift. The latter was calculated by FEFF8 and the fit was done by minimizing the k^3 weighted difference $[k\chi_{exp}(k) - k\chi_{calc}(k)]^2$.

As the main contribution to the EXAFS signal comes from the single scattering, we first attempted to fit the EXAFS parameters describing this contribution for the LT sample in R-space from 1.9 to 3.8 Å. We used four parameters: a global parameter R, a global thermal factor σ^2, a global energy shift parameter dE and an occupation factor S02_1; the results obtained are listed in Table 2. From the results of this calculation, it appears that the radius of the C_{60} cage measured by EXAFS is close to the expected value. On the other hand, the occupation factor is weak, but this might be due to signal reduction effects coming, for example, from multielectronic excitations. However, the shape of the experimental signal in R-space suggests that the single-scattering contribution is not fully separated from the multiscattering ones (Figure 4). The MS contributions were analyzed in two steps in order to fit the signal in R-space between 1.9 and 4.7 Å. First, only paths 2 and 3 of Table 1 were taken into account together with the single-scattering contribution. For this calculation only one free parameter was added, S02_2, a global occupation factor associated to all the MS contributions. The result of the fit is given in the Supporting Information, and the calculated parameters are reported in Table 2. The main change related to the description of the single-scattering contribution concerns the occupation factor S02_1 which is now close to 1; this means that some destructive interference occurs between the single-scattering and the first MS contributions. The value found for S02_2 is a little high and has to be considered with caution because the two first MS contributions are clearly not sufficient to describe the MS peaks (from 3.8 to 4.7 Å). Therefore, we include all the three- and four-legged paths' MS contributions up to 5.5 Å (paths 2−20 of Table 1) in the calculation.

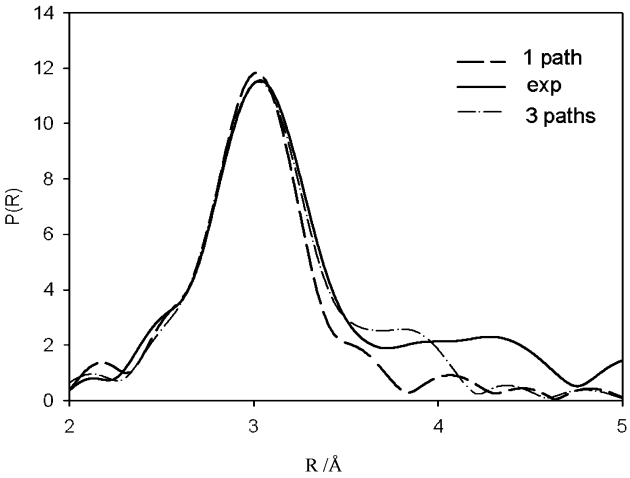

Figure 4. EXAFS data and fit of the LT sample with one and three paths.

Surprisingly, this does not improve significantly the fit in the MS region. Depending on the number of paths included, S02_2 may be reduced, but there is no satisfactory criterion to choose a particular value. The difficulty in fitting the MS signals is likely due to their high number. If the occupation and thermal factors of each path are considered as free parameters, they exceed the number of independent parameters ($1 + 2\Delta k\Delta R/\pi < 10$ for the MS contributions in the present case) which may be fitted. On the other hand, the use of global occupation and thermal factors may be too crude an approximation.

By comparing the data obtained for samples RT and LT (Figure 2) one can see that the main peak in the RT sample is about 60% in height compared to that of the LT sample. Because no change in the coordination number has occurred, one should obtain the same coordination number, within the experimental errors, and a higher thermal factor. The analysis performed for these data suggested instead that the thermal factor is similar but the coordination number is smaller (see Table 2). These results cannot be easily explained; one possibility would be the existence of an anharmonic movement, but then the Kr−C distance obtained in the fit would have been affected by this movement, by underestimating its value.[21] By considering the fact that we analyzed a molecular structure, hence no change in the coordination number took place, we set the value of S02_1 as 1.0 and analyzed all the other parameters as was done for the LT sample, (see parts a and b of Figure 5 and Table 2). These values are similar to those obtained for the LT sample, with the exception of the thermal parameter σ^2 whose value became rather large, that is, 0.013 Å^2. We assume that this behavior is due to a high-speed rotation of the C_{60} cage. In contrast to usual solids in which the disorder is associated with atomic vibrations, in Kr@C_{60} a rotation of the C_{60} molecule has to be considered. On the basis of powder X-ray diffraction

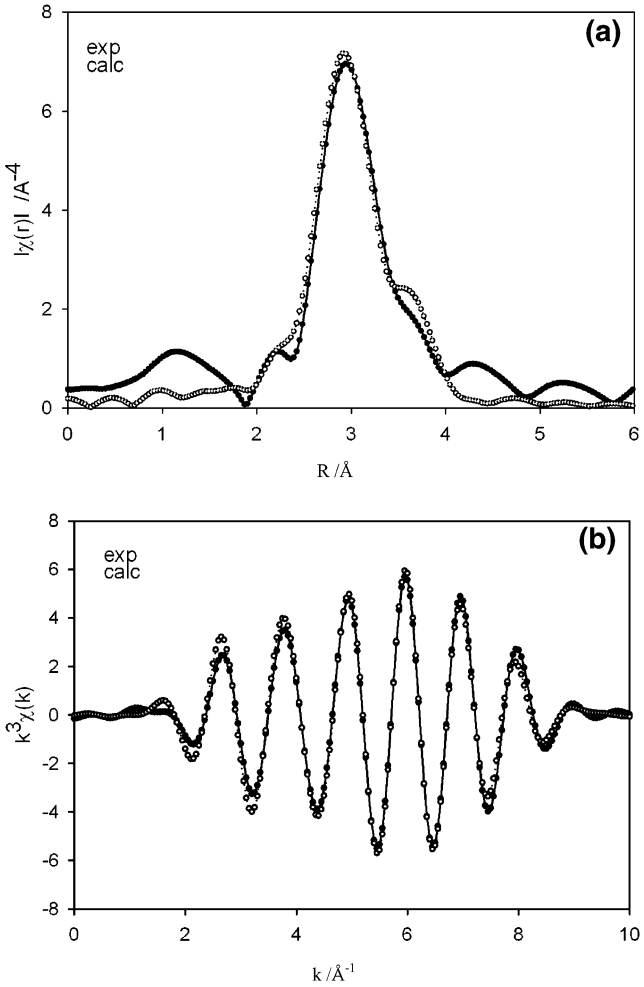

Figure 5. (a) EXAFS data and fit of the RT sample; the occupation factor for the first shell is fixed to unity. (b). The *k*-space representation of the filtered EXAFS signal contribution for the RT sample.

performed on a film of Kr@C_{60}, we found that the crystal structure of pure Kr@C_{60} is similar to that of empty C_{60}. Moreover, both compounds have the same molecular structure as determined by single-crystal X-ray crystallography,[20] and there is only a van der Waals interaction between the cage and the Kr atom, as seen from their spectroscopic properties.[19] In the solid state C_{60} molecules are freely rotating above 260 K, without correlation between the rotation directions.[22] Above this temperature, in the face-centered cubic (fcc) crystal structure,[23] C_{60} can be regarded as a sphere.[24−26] Below 260 K, C_{60} rotates only in two directions, and the energy difference between the two is only 11 meV;[27] thus, C_{60} can "jump" between these two states because of the low rotating potential energy. It is only below 90 K that C_{60} solid freezes.[23]

This rotation of the cage can affect the results of classical analysis; it introduced some anisotropy in the system because a photoelectron emitted along the rotation axis experiences a lower thermal disorder than a photoelectron emitted in a perpendicular direction.

As for the multiple scattering, the rotation of the cage will imply the diminution of the multiple scattering contribution by the distribution of their distances; the rotation acts in the same way as a disorder thus adding to the "natural" thermal displacements. Therefore MS peaks at room temperature should be weaker and broader than at low temperature when the rotation diminishes, which is the case observed.

We assume that EXAFS data at RT describe the rotating state of C_{60}, whereas those at LT describe the stillness state of C_{60}. The Kr@C_{60} rotation behavior should be similar to that of empty C_{60} because no interactions exist between the cage and the intercalant. This should be in agreement with our EXAFS data, at least concerning the multiple scattering contribution. More work is needed, in particular at different temperatures, to clarify the effect of the rotation on the EXAFS signal.

In conclusion, our data show clearly the endohedral character of this system, determine the radius of the cage, and infer that a peculiar effect such as high-speed rotation may affect the EXAFS signal.

Conclusion

In this report we discuss a rare set of Kr K-edge EXAFS data of Kr@C_{60} measured at 80 and 300 K. By analyzing experimental data obtained at the Kr K-edge, we conclude that the rotation of the cage takes place at room temperature similar to the case of pristine C_{60}. A freezing or at least a dramatic decrease in the rotation of the cage may explain the increase of the multiple scattering peaks at low temperature. As known from other spectroscopic techniques, the data confirm the endohedral character of the molecule as well as the insensitivity of the cage dimension to temperature. We can see Kr EXAFS spectroscopy as a local probe of the C_{60} structure and symmetry, acting from the interior of the fullerene.

Acknowledgment. We thank Agnès Traverse of LURE, University of Paris XI, Orsay, for all the help provided during these experiments. We also thank the Japan Science and Technology Corporation for financial support (SORST program) and the U.S. National Science Foundation for a Grant (CHE-0307168) provided to M.S. and R.J.C.

Supporting Information Available: EXAFS data and fit for the LT sample (three paths). This material is available free of charge via the Internet at http://pubs.acs.org.

References and Notes

(1) (a) Kroto, H. W.; Heath, J. R.; O'Brien, S. C.; Curl, R. F.; Smalley, R. E. *Nature* **1985**, *318*, 162−163. (b) Heath, J. R.; O'Brien, S. C.; Zhang, Q.; Liu, Y.; Curl, R. F.; Kroto, H. W.; Tittel, F. T.; Smalley, R. E. *J. Am. Chem. Soc.* **1985**, *107*, 7779−7780.

(2) Johnson, R. D.; Vries, M. S.; Salem, J.; Bethune, D. S.; Yannoni, C. S. *Nature* **1992**, *355*, 239−240.

(3) Weaver, J. H.; Chai, Y.; Kroll, G. H.; Jin, C.; Ohno, T. R.; Haufler, R. E.; Guo, T.; Alford, J. M.; Conceicao, J.; Chibante, L. P. F.; Jain, A.; Palmer, G.; Smalley, R. E. *Chem. Phys. Lett.* **1992**, *190*, 460−464.

(4) Tanaka, M.; Umeda, B.; Nishibori, E.; Sakata, M.; Saito, Y.; Ohno, M. Shinohara, H. *Nature* **1995**, *377*, 46−49.

(5) Shinohara, H.; Yamaguchi, H.; Hayashi, N.; Sato, H.; Ohkohchi, M.; Ando, Y.; Saito, Y. *J. Phys. Chem.* **1993**, *97*, 4259−4261.

(6) Kikuchi, K.; Suzuki, S.; Nakao, Y.; Nakahara, N.; Wakabayashi, T.; Shiromaru, H.; Saito, K.; Ikemoto, I.; Achiba, Y. *Chem. Phys. Lett.* **1993**, *216*, 67−71.

(7) Murphy, T. A.; Pawlik, T.; Weidinger, A.; Höhne, M.; Alcala, R.; Spaeth, J.-M. *Phys. Rev. Lett.* **1996**, *77*, 1075−1078.

(8) Knap, C.; Weiden, N.; Kass, H.; Dinse, K.-P.; Pietzak, M.; Waiblinger, M.; Weidinger, A. *Mol. Phys.* **1998**, *95*, 999.

(9) Saunders, M.; Jiménez-Vàzquez, H. A.; Cross, R. J.; Poreda, R. J. *Science* **1993**, *259*, 1248−1430.

(10) Saunders, M.; Cross, R. J.; Jiménez-Vàzquez, H. A.; Shimshi, R.; Khong, A. *Science* **1996**, *271*, 1693−1697.

(11) Ruttimann, M.; Haldimann, R. F.; Isaacs, L.; Diedrich, F.; Khong, A.; Jiménez-Vàzquez, H.; Cross, R. J.; Saunders, M. *Chem.−Eur. J.* **1997**, *3*, 1071−1076.

(12) Saunders, M.; Jiménez-Vàzquez, H. A.; Cross, R. J.; Mroczkowski, S.; Gross, M. L.; Giblin, D. E.; Poreda, R. J. *J. Am. Chem. Soc.* **1994**, *116*, 2193−2194.

(13) Suetsuna, T.; Dragoe, N.; Harneit, W.; Weidinger, A.; Shimotani, H.; Ito, S.; Takagi, H.; Kitazawa, K. *Chem. Eur. J.* **2002**, *8*, 5079−5083.

(14) Suetsuna, T.; Dragoe, N.; Shimotani, H.; Takeda, A.; Ito, S.; Cross, R. J.; Saunders, M.; Takagi, H.; Kitazawa, K. *Fullerenes, Nanotubes, Carbon Nanostruct.* **2002**, *10*, 15−21.

(15) Newville, M. *J. Synchrotron Radiat.* **2002**, *8*, 322−324.

(16) Ankudinov, A. L.; Ravel, B.; Rehr, J. J.; Conradson, S. D. *Phys. Rev.* **1998**, *B58*, 7565.

(17) Cicco, A. D.; Filipponi, A.; Itié, J. P.; Polian, A. *Phys. Rev. B* **1996**, *54*, 9086−9098.

(18) Wulf, R.; Calas, G.; Ramos, A.; Büttner, H.; Roselieb, K.; Rosenhaur, M. *Am. Mineral.* **1999**, *84*, 1461−1463.

(19) Yamamoto, K.; Saunders, M.; Khong, A.; Cross, R. J.; Grayson, M.; Gross, M. L.; Benedetto, A. F.; Weisman, R. B.: *J. Am. Chem. Soc.* **1999**, *121*, 1591−1596.

(20) Lee, H. M.; Olmsted, M. M.; Suetsuna, T.; Shimotani, H.; Dragoe, N.; Cross, R. J.; Kitazawa, K.; Blach, A. L. *Chem. Commun.* **2002**, 1352−1353.

(21) Eisenberger, P.; Browm, G. S. *Solid State Commun.* **1979**, *29*, *6*, 481−484.

(22) Blinc, R.; Seliger, J.; Dolisek, J.; Arcon, D. *Phys. Rev. B* **1994**, *49*, 4993−5002.

(23) In the solid-state C_{60} has a fcc structure; see, for instance, (a) David, W. I. F.; Ibberson, R. M.; Matsuo, T. *Proc. R. Soc. London, Ser. A* **1993**, *442*, 129−146. But it can also crystallize in a hexagonal compact structure, see (b) Céolin, R.; Tamarit, J. L.; López, D. O.; Barrio, M.; Agafonov, V.; Allouchi, H.; Moussa, F.; Szwarc, H. *Chem. Phys. Lett.* **1999**, *314*, 21−26.

(24) Tycko, R.; Haddon, R. C.; Dabbagh, G.; Giarum, S. H.; Douglassc, D. C.; Mujsce, A. M. *J. Phys. Chem.* **1991**, *95*, 518−520.

(25) Chow, P. C.; Jiang, X.; Reiter, G.; Wochner, P.; Moss, S. C.; Axc, J. D.; Hanson, J. C.; McMiullan, R. K.; Meng, R. L.; Chu, C. W. *Phys. Rev. Lett.* **1992**, *69*, 2943−2946.

(26) Newmann, D. A.; Copley, J. R. D.; Cappelletti, R. L.; Kamitakahara, W. A.; Lindstrom, R. M.; Creegan, K. M.; Cox, D. M.; Romanow, W. J.; Coustel, N.; McCauley, J. P., Jr.; Maliszewskiyj, N. C.; Fischer, J. E.; Smith, A. B. *Phys. Rev. Lett.* **1991**, *67*, 3808−3811.

(27) Prassides, K. *Phys. Scr., T* **1993**, *49*, 735.